

# THE THERMAL HISTORY OF THE STEINACH NAPPE (EASTERN ALPS) DURING EXTENSION ALONG THE BRENNER NORMAL FAULT SYSTEM INDICATED BY ORGANIC MATURATION AND ZIRCON (U-TH)/HE THERMOCHRONOLOGY

N. Keno LÜNSDORF<sup>1)</sup>, István DUNKL<sup>1)</sup>, Burkhard C. SCHMIDT<sup>2)</sup>, Gerd RANTITSCH<sup>3)</sup> & Hilmar von EYNATTEN<sup>1)</sup>

<sup>1)</sup> Dept. of Sedimentology & Environmental Geology, Geoscience Center Georg-August-Universität Göttingen, Germany;

<sup>2)</sup> Dept. of Experimental & Applied Mineralogy, Geoscience Center Georg-August-Universität Göttingen, Germany;

<sup>3)</sup> Department of Applied Geosciences and Geophysics, University of Leoben, Austria;

<sup>†</sup> Corresponding author, keno.luensdorf@geo.uni-goettingen.de

## KEYWORDS

Raman spectroscopy of organic matter  
Brenner Normal Fault  
Thermochronology  
Steinach Nappe  
Eastern Alps

## ABSTRACT

During the Miocene, the Brenner Normal Fault displaced the Austroalpine Steinach Nappe together with its underlying, tectonically thinned Austroalpine units from the tectonically underlying Penninic basement. The thermal effects of the displacement on the hanging wall were studied by geothermometry using Raman spectroscopy of carbonaceous material, vitrinite reflectance and by zircon (U-Th)/He thermochronology in a section through the Steinach Nappe. The results show that the hanging wall remained thermally unaffected by Miocene extension. The last thermal overprint of the Upper Carboniferous sediments of the Steinach Nappe took place during Late Cretaceous tectonic burial, resulting in metamorphic peak temperatures of ~300 °C to ~350 °C.

Die Ostalpine Steinacher Decke wurde zusammen mit den unterlagernden, tektonisch ausgedünnten Ostalpinen Decken während des Miozäns entlang der Brenner Störungszone vom tektonisch unterlagernden Penninikum abgeschoben. Der thermische Einfluss auf den hangenden Block dieser Abschiebung wurde in einem Profil durch die Steinacher Decke mittels Raman Spektroskopie der organischen Substanz, Vitrinit Reflexion und Zirkon (U-Th)/He Thermochronologie untersucht. Die Ergebnisse zeigen, dass die miozäne Extension den hangenden Block thermisch nicht beeinflusst hat. Die letzte thermische Überprägung der oberkarbonischen, sedimentären Abfolge der Steinacher Decke fand während der spät kretazischen, tektonischen Versenkung statt, die eine metamorphe Maximaltemperatur von etwa 300 °C bis ca. 350 °C zur Folge hatte.

## 1. INTRODUCTION

Extension along large scale shear zones due to footwall exhumation is accompanied by heat advection and fluid circulation which leads to a perturbation of isotherms and a thermal overprint of the hanging wall (e.g. Grasemann and Mancktelow, 1993; Dunkl et al., 1998). Consequently, Rantitsch et al. (2004, 2005) proposed that low- to very low-grade metamorphic hanging wall units at the eastern segment of the Eastern Alps (Graz Palaeozoic and Eastern Greywacke Zone), tectonically overlying decompressed middle- to high-grade metamorphic rocks, were overprinted by advective heat and convective fluids during Late Cretaceous to Palaeogene times. From the metamorphic pattern of the central Western Greywacke Zone, Rantitsch and Judik (2009) concluded that this effect acted also during the Miocene rapid exhumation of formerly deeply buried rocks of the Penninic Unit, exposed in the Tauern Window.

The Austroalpine Steinach Nappe formed the highest unit of the Austroalpine hanging wall during the Miocene activity of the Brenner Normal Fault system (BNF; Fig. 1; Fügenschuh et al., 2000). Greenschist to amphibolite facies Penninic formations were exhumed along the BNF in a rather short time period (Selverstone et al., 1995; Fügenschuh et al., 1997; Neubauer et al., 1999), thus the advective heat transfer from the

footwall may have affected the hanging wall. In order to quantify the syn-extensional thermal history of the hanging wall above a prominent detachment of the Eastern Alps we have performed a combined study of organic maturation indices (Raman spectroscopy of carbonaceous material and vitrinite reflectance) and low temperature thermochronometry (zircon (U-Th)/He dating).

## 2. GEOLOGICAL SETTING

The Tauern Window of the Eastern Alps is composed of two nappe systems (Frisch, 1980). The tectonically lower Venediger Nappe is composed of polymetamorphic European-derived basement and a Permian to Mesozoic cover (Lower Schieferhülle). The upper nappe system (Glockner Nappe – Matriere nappe system in Figure 1) consists of Triassic sequences, Bündner Schiefer and ophiolites (Frisch, 1980). The Tauern Window was affected by at least three metamorphic events, in eclogite, blueschist and greenschist to amphibolite facies (Hoinkes et al., 1999). Of these three events, the greenschist to amphibolite facies metamorphism ('Tauernkristallisation') is the youngest one and affected the entire Tauern Window, increasing in degree from the periphery to the central parts of the window (Hoinkes et al., 1999).

The western margin of the Tauern Window is marked by the Miocene Brenner Normal Fault system which displaced the Austroalpine nappe stack from the Penninic units of the Tauern Window. Following Schmid et al. (2004), the Austroalpine is represented here by the upper three nappes of the Upper Austroalpine basement nappes. The basal Ötztal-Stubai basement complex (OSK) underwent a polymetamorphic evolution in which the youngest (Eoalpine) metamorphic event is of Cretaceous age (Fügenschuh et al., 2000). This event resulted in a metamorphic gradient from lower greenschist facies in the NW to upper amphibolite facies in the southeast of the OSK.

The Brenner Mesozoic (BM) forms the immediate sedimentary cover sequence of the OSK. The Steinach and Blaser Nappes above were thrust over the BM by Eoalpine tectonics (Fig. 1). The Steinach Nappe consists predominantly of quartzphyllites (Oberbergthal-Subnappe and Gschnitztal-Subnappe in Figure 1), which are overlain by a probably transgressive series of weakly metamorphosed Upper Carboniferous silici-

clastic sediments (Schulz and Fuchs, 1991; Fig. 1). Quartz conglomerates and coarse quartzarenites prevail in these series (Krainer, 1990). Intercalations of pelites are common, as well as anthracitic coal seams (Krainer, 1990, Schulz and Fuchs, 1991).

The rapid Miocene exhumation of the Tauern Window (Fügenschuh et al., 2000) was accompanied by tectonic unroofing and thus lateral extrusion and disintegration of the Austroalpine cover units (Frisch et al., 2000). At the western boundary of the Tauern Window exhumation was compensated by the BNF (Behrmann, 1988; Selverstone, 1988; Fügenschuh et al., 1997; Frisch et al., 2000; Reiter et al., 2005). This low angle normal shear zone strikes roughly N-S (Fig. 1). In its northern part (Silltal Fault), the fault zone is purely brittle and juxtaposes structurally lower Austroalpine basement in the footwall beside structurally higher Austroalpine in the hanging wall (Fügenschuh et al., 1997; Rosenberg and Garcia, 2011). The southern part (Brenner Fault s. s.) is a westward dipping mylonite belt em-

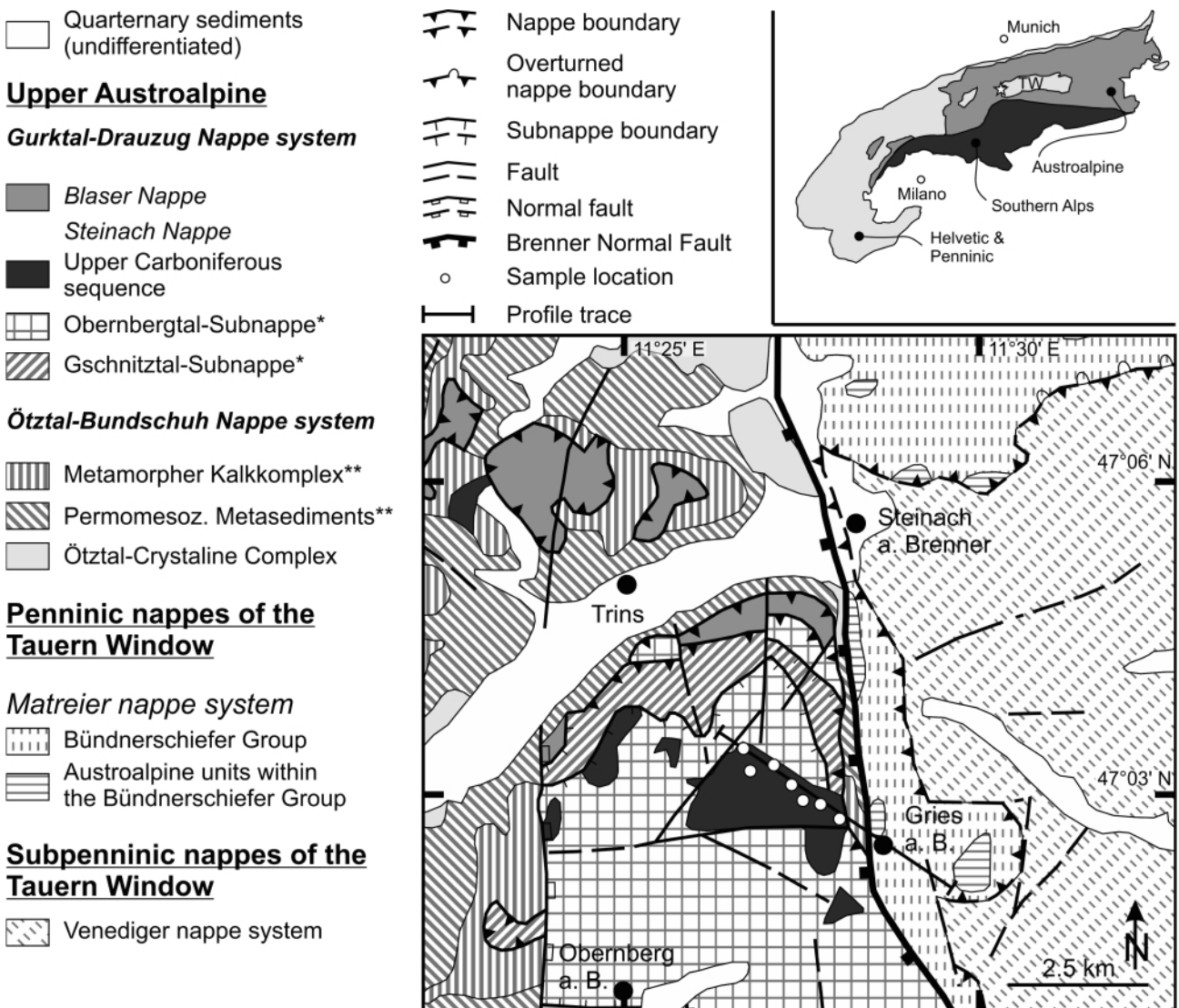


**FIGURE 1:** The inset shows the major structural units of the Alps. A star indicates the study area at the western termination of the Tauern Window (TW). The simplified geological map of the working area shows the major geological units, the sample localities and the profile trace. \*) These subnappes together form the Steinacher Quartzphyllite. \*\*) Together these units form the Brenner Mesozoic (BM). (after Rockenschaub & Nowotny, 2009)

placing the Upper Austroalpine units (Ötztal-Stubai basement complex, Brenner Mesozoic, Steinach Nappe and Blaser Nappe) beside the Penninic units of the Tauern Window (Fügenschuh et al., 1997; Rosenberg and Garcia, 2011).

Ar-Ar-dating of white mica from metapelites of the Steinach Nappe resulted in Variscan cooling ages (321 – 311 Ma, Rockenschaub et al., 2003). Further muscovite Ar-Ar-ages from the BM and OSK are in the range of 100 – 80 Ma (Frank et al., 1987; Elias, 1998; Rockenschaub et al., 2003), indicating an Eoalpine thermal overprint.

Low temperature thermochronological data suggest that the Austroalpine units of the BNF hanging wall were already exhumed to a depth as shallow as ~4 km during the onset of exhumation of the Tauern Window ca. 20 Ma ago (Fügenschuh et al., 1997). At that time, the Penninic units of the footwall were still at a depth of ~23 to 25 km, indicating a total vertical displacement of ~20 km along the BNF (Selverstone et al., 1995; Fügenschuh et al., 1997, 2000). However, according to Rosenberg and Garcia (2011) the exhumation of the Tauern Window was not only due to extensional unroofing but comprises a combined effect of folding in the footwall and erosion. Their calculations point toward a vertical displacement of only ~5 km at the BNF resulting in an extensional displacement of 2 to 14 km.

### 3. METHODS AND SAMPLE PREPARATION

#### 3.1 SAMPLING

The Upper Carboniferous sedimentary series within the Stein-

ach Nappe adjacent to the recent contact between Austroalpine and Penninic rocks contains organic rich pelites embedded in coarser siliciclastic rocks, thus providing ideal sample material for the methods applied in this study. Samples were collected in the Upper Carboniferous sequence of the Steinach Nappe along a SE-NW profile (see Figs. 1 and 2). Various coal mining dumps allowed the collection of fresh, organic rich material. Pelites and metapelites with high organic content were selected for Raman spectroscopy of carbonaceous material and vitrinite reflectance measurements, while quartz-rich sandstones were taken from the same sampling locations for zircon (U-Th)/He-measurements. Table 1 shows the geographical coordinates of all samples, their petrography and the applied analytical methods.

#### 3.2 SAMPLE PREPARATION

The sandstone samples were crushed by a jaw crusher and the <250 µm fraction was pre-concentrated by a Wilfley table. The pre-concentrated heavy mineral rich fractions were etched by 5% acetic acid for max. 3 days to remove the carbonate grains and clay-carbonate-iron oxide coatings. Heavy minerals were separated by sodium-polytungstate solution (density of 2.84 g/cm<sup>3</sup>). A Franz isodynamic separator was used in five steps to concentrate the zircon grains in the low-susceptibility mineral fraction.

Samples for Raman analysis were treated chemically to dissolve all other mineral phases except the organic (see Rantitsch et al., 2004). These samples were crushed to chips of 5 to 10 millimeters. The rock-chips were initially bathed for two

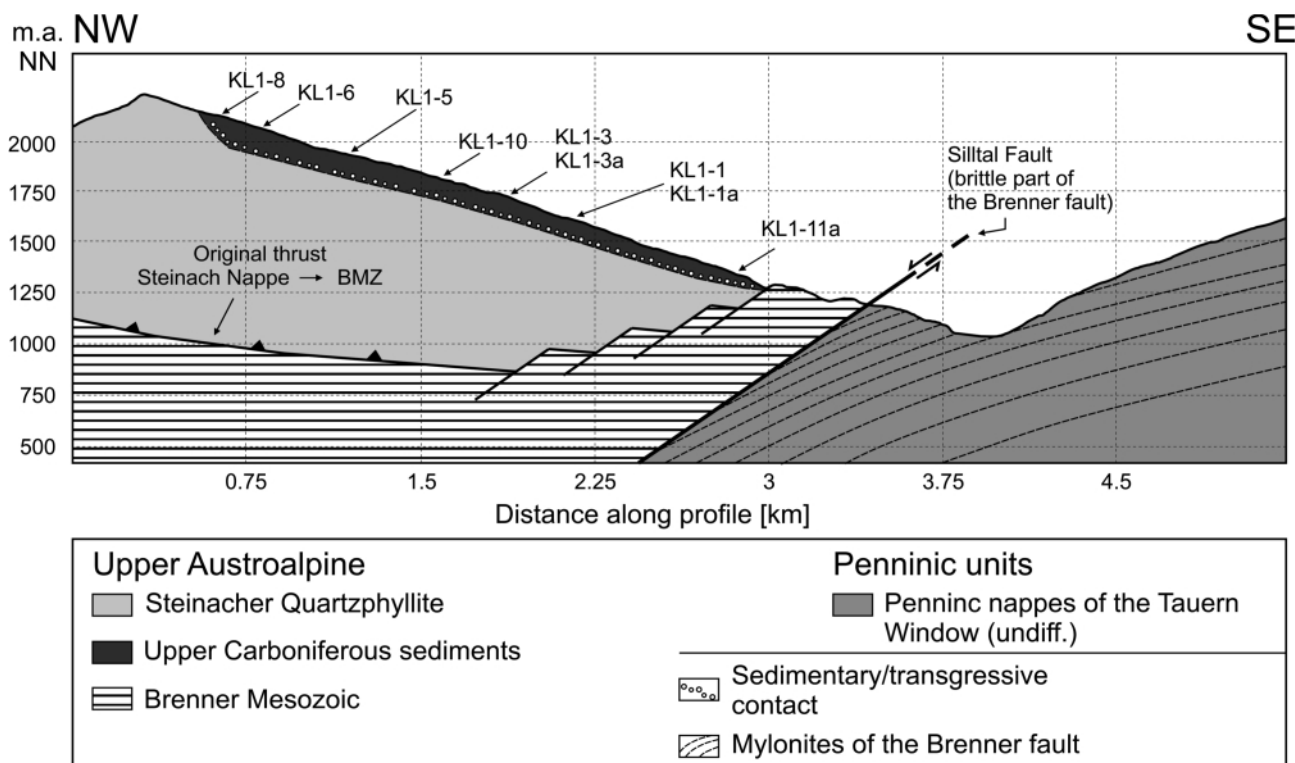


FIGURE 2: Schematic sketch of NW-SE section across the Brenner Fault, including approximate sampling locations (for location of the profile see Fig. 1) and the major geological units.

days in a 1:1 solution of 37% hydrochloric acid to dissolve carbonates. After HCl-treatment, the samples were mixed with 1:1 diluted 48% hydrofluoric acid. After hydrofluoric acid treatment the sample suspensions were decanted until the pH-value of 5 to 6 was reached. Remaining fluids were evaporated in a drying oven at 50 °C. About 10 to 20 mg of the dried carbonaceous material were mixed with 1 - 2 ml de-ionized water in a small glass vial and put into an ultrasonic bath for about 60 seconds in order to disperse the carbonaceous material.

For the Raman analysis, the suspension was then deposited and dried on a glass slide.

### 3.3 ANALYTICAL METHODS

On sections cut perpendicular to the foliation, the rank of organic maturation was determined by measurement of the maximum and minimum organic matter reflectance ( $R_{max}$ ,  $R_{min}$ ) under oil immersion in polarized light at a wavelength of 546 nm.

Raman spectra were obtained using a Horiba Jobin Yvon HR800-UV spectrometer with an attached Olympus BX-41 microscope and a 100x long working distance objective with a numerical aperture of 0.8. An Ar<sup>+</sup>- laser with a wavelength of 488 nanometers with output power of 20 mW was used as excitation source. To avoid sample alteration due to heating, density filters attenuated the laser beam to ~0.3 mW at the sample. A holographic grating with 600 grooves per millimeter was used for diffraction and a Peltier element cooled CCD detector recorded the diffracted light. Spectra were measured in one spectral window in 15 seconds.

After linear baseline correction, spectral curve fitting was performed with the open source software Fityk (Wojdyr, 2010) following a strict fitting-protocol (Lünsdorf, 2010) to reduce the variation in the fitting results due to spectral evaluation. This protocol involves subsequent fitting Lorentzian functions to the Raman bands (D1, D2, D3, D4, G; see Fig. 3). The spectra were also evaluated numerically according to the evolution of Raman spectra of carbonaceous material in the temperature range of ~200 to ~320 °C as described by Lahfid et al. (2010). Accordingly the spectra evolve as follows:

1. The D1-band is more intense than the G-band at temperatures higher than 300 °C and less intense below 300 °C.
2. From ~230 °C to ~300 °C the relative intensity of the D1-band increases, while the intensity of the D4-band decreases.
3. At about 250 °C the intensity of the D4-band is roughly half the intensity of the composite D-band.
4. Below 250 °C the D4-band becomes a distinct feature.
5. The G-band is asymmetric towards the high wavenumber

Sample	Latitude	Longitude	Elevation (m)	Petrogr.	RSCM	VR	ZHe
KL1-1	47°2'57.74"N	11-27'37.60"E	1705	pelite	x	x	
KL1-1a	47°2'57.74"N	11-27'37.60"E	1705	sst			x
KL1-3	47°3'0.80"N	11-27'26.78"E	1790	pelite	x	x	
KL1-3a	47°3'0.80"N	11-27'26.78"E	1790	sst			x
KL1-5	47°3'19.50"N	11-26'57.96"E	2010	pelite-sst	x		
KL1-6	47°3'17.87"N	11-26'47.65"E	2067	pelite	x	x	
KL1-8	47°3'25.16"N	11-26'41.65"E	2130	sst			x
KL1-10	47°3'6.77"N	11-27'16.29"E	1865	pelite	x	x	
KL1-11a	47°2'44.91"N	11-28'4.41"E	1475	congl.	x		x

**TABLE 1:** Sample list showing the petrography, analytical methods for each sample and the coordinates of the sampling locations (Petrogr. = Petrography, Raman = Raman spectroscopy of carbonaceous material, ZHe = zircon (U-Th)/He thermochronology). sst = sandstone, congl. = conglomerate

side above 300 °C, symmetrical between 200 °C and 300 °C and slightly asymmetric towards the low wavenumber side below 200 °C.

Lahfid et al. (2010) proposed two Raman-peak ratios that increase with increasing peak metamorphic temperature. These ratios are:

$$RA1 = \frac{(D1 + D4)_{area}}{(D1 + D2 + D3 + D4 + G)_{area}} \quad (1)$$

$$RA2 = \frac{(D1 + D4)_{area}}{(D2 + D3 + G)_{area}} \quad (2)$$

However, as the applied laboratory setup is different to the setup of Lahfid et al. (2010) only their qualitative description was used to determine temperature. Considering, that the peak-height ratio of the D- and G-band increases with increasing excitation wavelength (Wang et al., 1990) it is likely that the Raman spectra obtained here underestimate temperature when the above stated qualitative description is used. As the difference in wavelength is only 26 nm (Lahfid et al. (2010): 514 nm, this study: 488 nm), it is assumed that the underestimation of temperature is minor.

For (U-Th)/He chronology, intact zircon crystals with a width > 75µm were carefully selected and individually wrapped in platinum capsules. The Pt capsules were heated up by an infrared laser for 7 minutes. The extracted gas was purified using a SAES Ti-Zr getter at 450 °C. The chemically inert noble gases and a minor amount of other rest gases were then expanded into a Hiden triple-filter quadrupol mass spectrometer. Helium blanks were estimated using the same procedure on empty Pt tubes (ca. 0.0003 and 0.0008 ncc <sup>4</sup>He, 'cold' and 'hot' blanks, respectively). Crystals were checked for degassing of He by sequential reheating and He measurement. Following degassing, the crystals were retrieved from the gas extraction line, spiked with calibrated <sup>230</sup>Th and <sup>233</sup>U solutions, and dissolved in HF + HNO<sub>3</sub> acid mixture in teflon bombs in five days. Spiked solutions were analyzed by a Perkin Elmer Elan DRC II ICP-MS with an APEX micro-flow nebulizer. Procedural U and Th blanks by this method are usu-

Sample	Elevation (m)	Rr	s.d.	Rmax	s.d.	Rmin	s.d.	N	Calc. Temp. (°C)
KL1-6	2067	1.41	0.16					30	182 - 212
KL1-10	1865	2.86*		3.44	0.37	2.35	0.44	30	276 - 300
KL1-3	1790	4.25*		5.56	0.55	2.86	0.86	30	329 - 349
KL1-1	1705	4.40*		5.81	0.56	2.61	0.96	14	334 - 353

**TABLE 2:** Vitrinite reflectance values for samples KL1-1, KL1-3, KL1-6 and KL1-10. The samples are listed according to their position in the profile from higher to lower position. Rr values with an asterisk are deduced from the Rmax values according to Koch and Guenther (1995). s.d. = standard deviation, N = number of measurements.

ally very stable in a measurement session and below 1.5 pg. Sm, Pt and Zr were determined by external calibration. The oxide formation rate and the PtAr - U interference was always monitored, but the effects of these isobaric argides were negligible relatively to the signal of actinides. The alpha ejection was corrected after Farley et al. (1996) and Farley (2002).

#### 4. RESULTS

Vitrinite reflectance values were acquired for four samples and maximum temperatures were estimated according to  $T (°C) = (\ln(Rr) + 1.2)/0.0078$  (Barker and Pawlewicz, 1986) (Tab. 2). The values decrease along the profile from bottom to top, indicating temperatures of about 350 °C at the base and about 200 °C at the top of the profile (Tab. 2).

Figure 3 shows representative Raman spectra of samples collected along the profile. The D1-band is always less intense than the G-band (except in KL1-11a where they are of equal intensity), the D4-band is never a distinct feature and the combined G+D2-band is nearly symmetrical. A clear trend is not evident in this series of spectra, but KL1-11a indicates the highest temperature (D1-band and G+D2 are of equal intensity and G+D2-band shows a slight asymmetry toward the high wavenumber side). Comparing the shape of the measured spectra with the change in shape of spectra from ~160 – 320°C given in figure 3 in Lahfid et al. (2010) all samples experienced a maximum temperature of ca. 250 °C to 300 °C.

The RA1 and RA2 ratios listed in Table 3 give nearly the same results. The RSCM-thermometer calibrated by Lahfid et al. (2010) delivers a temperature range of ca. 290 – 300°C and shows no trend along the profile. For reasons stated above

Sample	n	RA1	1 s.d.	RA2	1 s.d.	T. Lahfid (°C)	1 s.d.
KL1-11a	30	0.61	0.01	1.58	0.04	295	7
KL1-1	30	0.62	0	1.61	0.03	301	6
KL1-3	30	0.61	0.01	1.59	0.04	297	7
KL1-10	30	0.62	0	1.62	0.03	303	5
KL1-5	30	0.61	0	1.55	0.02	290	5
KL1-6	30	0.61	0.02	1.59	0.2	296	28

**TABLE 3:** Raman spectroscopic data of carbonaceous material from the Steinach Nappe. The samples are listed according to their position in the profile, sorted from bottom to top. N = number of spectra, s.d. = standard deviation, RA1 and RA2 = Peak-ratios after Lahfid et al. (2010).

this calculated temperature range should only be used as temperature estimation. Nevertheless, it can be deduced from the Raman measurements that the Carboniferous sequence reached a maximum temperature of about 300°C, which is in accord with the vitrinite data.

(U-Th)/He ages were retrieved for three samples because suitable zircon crystals were rare in most samples

(see details in Table 4). However, the analyzed samples cover nearly the entire length of the exposed Steinach Nappe: KL1-11a derived from the base, KL1-1a from the middle part and KL1-8 from the uppermost part of the profile (Fig. 2). The ZHe ages range from 70 Ma to 63 Ma with the youngest ages in the middle section of the profile, providing that there is no trend in cooling ages.

#### 5. DISCUSSION

The Ar-Ar ages of 321 to 311 Ma of white mica from the basement of the Steinach Nappe (Steinach Quartzphyllite) were interpreted as post-Variscian cooling ages (Rockenschaub et al., 2003). The Carboniferous sequence of the Steinach Nappe is supposedly transgressively covering the Steinach Quartzphyllite and is biostratigraphically dated as Westfal D (Upper Moskovian to Lower Kasimovian, ~ 307 – 304 Ma; Krainer, 1990, 1992). Consequently, the basement of the Steinach Nappe must have been exhumed to the surface in a period of about 320 Ma to ca. 306 Ma. Subsequent to sedimentation, the Carboniferous sequence was buried due to deposition of Permo-Mesozoic strata, today partly exposed within the Blaser Nappe. Schulz and Fuchs (1991) give a maximum burial depth of 4000 to 5000 m for the Carboniferous sequence. Figure 4 shows the compiled thermal history of the OSK and the Carboniferous sequence of the Steinach Nappe.

During Late Cretaceous the Steinach Nappe was thrust together with its cover (Blaser Nappe) over the Brenner Mesozoic and Ötztal Stubai basement complex. The Austroalpine units experienced Eoalpine metamorphism, which climax was dated to  $90 \pm 10$  Ma (Frank et al., 1987). The thickening was followed by extension between ca. 80 and 67 Ma (Froitzheim et al., 1997).

Due to its higher structural position, the Steinach Nappe was less affected by the Eoalpine event, as shown by the preservation of Variscian white mica Ar-Ar ages (Rockenschaub et al., 2003), which indicates an Eoalpine maximum temperature of about 350 °C to 400 °C for the Steinach Nappe. This temperature limit is affirmed by the degree of organic maturation that yields maximum temperatures of >300 °C (RSCM) to ~350 °C (VR). The underlying Brenner Mesozoic underwent a higher Eoalpine metamorphic overprint with peak temperatures of ~500 °C (Fügenschuh et al., 2000) at 100 – 80 Ma (Rockenschaub et al., 2003).

Supposedly during Late Cretaceous extension, the Blaser

Nappe was detached from the Steinach Nappe. This phase is very likely represented by the increased exhumation rate of

the OSK and its cover units from about 90 Ma to ca. 60 Ma (Fügenschuh et al., 2000). The ZHe-ages provided herein (70

Sample	aliq.	He		U238			Th232			Th/U	Sm			Ejection	Uncorr.	Ft-Corr.	1s	Sample unweighted average & s.e.	
		vol.	s.e.	mass	s.e.	conc.	mass	s.e.	conc.		mass	s.e.	conc.	correct.	He-age	He-age			
		[ncc]	[%]	[ng]	[%]	[ppm]	[ng]	[%]	[ppm]	ratio	[ng]	[%]	[ppm]	(Ft)	[Ma]	[Ma]	[Ma]		
KL1-8 (2130 m)	#1	17.9	1.6	2.28	1.8	431	0.99	2.4	187	0.43	0.05	13	10	0.77	58.7	75.7	3.1	70.6	10.4
	#2	10.9	1.6	1.35	1.8	228	0.57	2.4	96	0.42	0.01	12	1	0.78	60.7	77.5	3.1		
	#3	23.57	1.6	4.32	1.8	1073	0.2	2.4	49	0.05	0.02	10	4	0.76	44.6	58.7	2.5		
KL1-1a (1705 m)	#1	2.78	1.7	0.5	1.8	227	0.14	2.4	62	0.27	0.01	11	5	0.73	43	59.3	2.8	63,2	7
	#2	5.06	1.7	0.81	1.8	420	0.09	2.4	44	0.11	0.01	11	4	0.72	50.3	69.8	3.4		
	#3	5.32	1.7	0.96	1.8	497	0.1	2.4	52	0.1	0.01	11	4	0.71	44.7	62.9	3.1		
	#4	2.4	1.7	0.36	1.9	143	0.13	2.4	51	0.36	0.02	11	9	0.71	50.1	70.3	3.5		
	#5	3.98	1.7	0.79	1.8	459	0.23	2.4	131	0.29	0.05	11	31	0.72	38.8	54	2.6		
KL1-11a (1475 m)	#1	7.09	1.7	1.07	1.8	179	0.23	2.4	38	0.21	0.01	20	1	0.74	52	70.5	3.2	70	0.5
	#2	22.39	1.6	3.12	1.8	407	0.74	2.4	97	0.24	0.02	12	2	0.81	56	69.4	2.6		
	#3	6.81	1.7	1.05	1.8	201	0.12	2.4	22	0.11	0.01	19	1	0.75	52.3	70.1	3.1		

**TABLE 4:** Zircon (U-Th)/He ages obtained on the Carboniferous sandstone samples of the Steinach Nappe. Amount of helium is given in nano-cubic-cm in standard temperature and pressure. Amounts of radioactive elements are given in nanograms. Ft: alpha-ejection correction (according to Farley, 2002). Error on average age is 1s, as (SD)/(n)(1/2); where SD=standard deviation of the age replicates and n=number of age determinations.

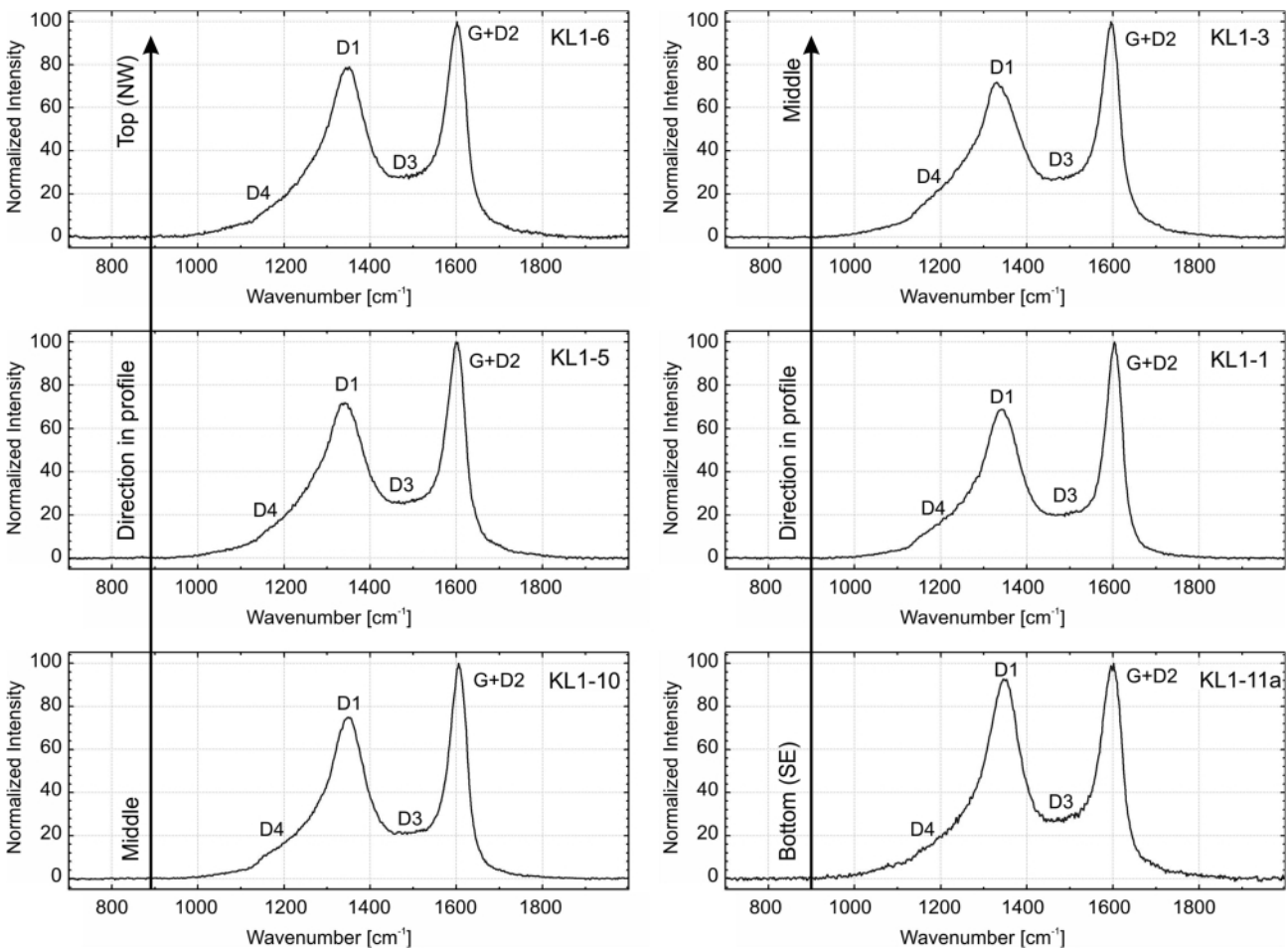


**FIGURE 3:** Representative Raman spectra of the 6 pelitic samples collected along the profile at the Steinach Nappe. The arrow indicates the relative position of the sample within the profile.

– 63 Ma) fit well in this scenario, because they are equal to the ZFT-ages of the BM as recorded by Fügenschuh et al. (1997, 2000). They demonstrate the tectonically higher position of the Steinach Nappe and imply that this nappe was exhumed together with the Brenner Mesozoic and Ötztal Stubai basement complex at a high cooling rate.

Since the Early Palaeogene, temperatures within the southern OSK were never higher than 100 – 200 °C (Fügenschuh et al., 2000), implying that the overlying units were even cooler. Considering that the Penninic units were contemporaneously at a depth of ~23 – 25 km (Fügenschuh et al., 1997) the isotherms within the hanging wall should have been perturbed by the rapid Miocene exhumation of the Tauern Window and an elevated temperature gradient could have been developed in the hanging wall of the BNF. In this case, both the RSCM data and vitrinite reflectance data at the base of the sampled profile should indicate increased temperatures while the (U-Th)/He-thermochronometer should be reset to Miocene ages when exhumation along the BNF was most intense.

Vitrinite reflectance indicates increasing temperatures along the profile from ~200 °C at the top to ~350 °C at the bottom (see Table 2). The RSCM-data (see Table 3 and Figures 3 and 4) do not give a temperature gradient, but a range from ~290 °C to ~300 °C. Thus, the organic maturation points to a vaguely increased temperature gradient within the Carboniferous sequence. However, the (U-Th)/He ages of 70 Ma to 63 Ma clearly show that the Carboniferous sequence was not overprinted above the reset temperature of the ZHe thermochronometer during the exhumation of the Tauern Window. Considering a ~10 million year maximum duration for the increased heat flow period generated by the exhumation along the BNF, the closure temperature of the ZHe thermochronometer is ca. 170 °C (Reiners, 2005). Therefore the maximum temperature registered by the organic maturation in the Carboniferous sequence was reached before the exhumation of the Penninic formations in Miocene times, very probably during Eoalpine nappe stacking and metamorphism.

Due to its structurally high position, the Steinach Nappe re-

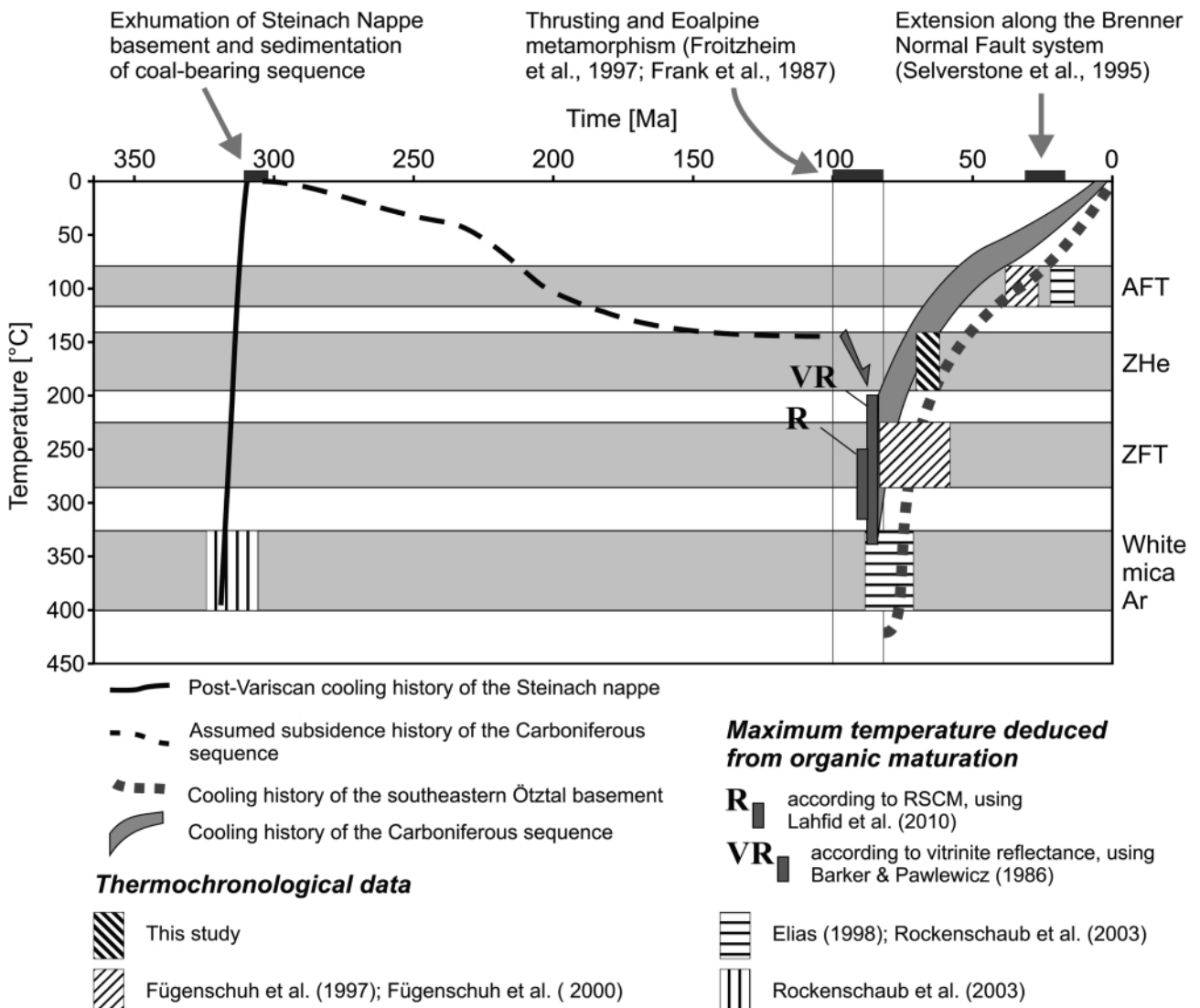


FIGURE 4: Time-temperature plot for the Ötztal-Stubai basement complex (+Brenner Mesozoic), Steinach Nappe and the Carboniferous sediments, integrating the new data, previously published thermochronological data, and major geological events.

mained thermally unaffected by the exhumation of the Tauern Window. At present, however, the sampled profile is in the immediate vicinity of the BNF; the deepest Carboniferous sample is situated as close as ca. 400 m to the Penninic footwall (see Fig. 2) and the ZHe thermochronometer shows no reset. Thus, it is assumed that the present geometry of the formations in the hanging wall of the BNF is the result of an extensional faulting that post-dated the major E-W displacement along the BNF. This probably Late Miocene faulting displaced the originally higher levels of the hanging wall to a much lower position and thus the deepest part of the Carboniferous strata are near-by the Penninic metamorphics.

## 6. CONCLUSIONS

The organic maturation indices reveal an increased thermal gradient and peak metamorphic temperatures of about 300 - 350 °C for the Carboniferous sequence of the Steinach Nappe. According to the new zircon (U-Th)/He ages detected of the same sample set the Carboniferous sequence experienced the thermal climax in Late Cretaceous time and remained thermally unaffected by the exhumation of the Tauern Window along the BNF. From this observation and formerly known data from Elias (1998), Fügenschuh et al. (1997, 2000), and Rockenschaub et al. (2003) the thermal history is deduced as follows (see Figure 4):

1. During the Early Carboniferous, the metamorphic basement of the Steinach Nappe (Steinach Quartzphyllite) was exhumed to the surface (white mica cooling ages: 321 to 311 Ma; according to Rockenschaub et al., 2003).
2. During the Lower Stephanian (Upper Moskovian to Lower Kasimovian), the Steinach Nappe basement was covered by the coal-bearing sedimentary sequence. Later, during Mesozoic times, a 4 to 5 km thick (Schulz and Fuchs, 1991) sedimentary pile accumulated on the Steinach Carboniferous, resulting in peak temperatures of ca. 170 to 190 °C.
3. During Eoalpine tectonics the Steinach Nappe was thrust upon the OSK and BM. The Upper Carboniferous sequence situated in the uppermost part of the Steinach Nappe and registered a thermal climax of ca. 300 - 350 °C due to tectonic burial.
4. During the latest Cretaceous, the OSK, BM and Steinach Nappe experienced rapid exhumation probably driven by extension.
5. During Miocene, the Tauern Window was exhumed rapidly, accompanied by extension along the BNF (Selverstone et al., 1995, Fügenschuh et al., 1997).
6. Post-exhumation faulting along the BNF displaced the Carboniferous sequence to the immediate vicinity of the Penninic metamorphics and now they are much closer to the Penninic formations than during active extension.

## ACKNOWLEDGEMENTS

We would like to thank B. Fügenschuh and K. Krainer for their constructive thoughts and reviews.

## REFERENCES

- Barker, C. E. and Pawlewicz, M., 1986. The Correlation of Vitrinite Reflectance with Maximum Temperature in Humic Organic Matter. *Lecture Notes in Earth sciences*, 5, Springer-Verlag Berlin Heidelberg, 79-93.
- Behrmann, J. H., 1988. Crustal-scale extension in a convergent orogen: the Sterzing-Steinach mylonite zone in the Eastern Alps. *Geodinamica Acta*, 2, 2, 63-73.
- Dunkl, I., Grasemann, B. and Frisch, W., 1998. Thermal effects of exhumation of a metamorphic core complex on hanging wall syn-rift sediments - an example from the Rechnitz Window, Eastern Alps. *Tectonophysics*, 297, 31-50.
- Elias, J., 1998. The Thermal History of the Oetztal-Stubai Complex (Tyrol, Austria/Italy) in the light of the Lateral Extrusion Model. *Tuebinger Geowissenschaftliche Arbeiten*, 42.
- Farley, K. A., 2002. (U-Th)/He dating: techniques, calibrations and applications, *Reviews in Mineralogy and Geochemistry*, 47, 819-844.
- Farley, K. A., Wolf, R. A. and Silver, L. T., 1996. The effects of long alpha-stopping distance on (U-Th)/He ages. *Geochim. Cosmochim. Acta*, 60, 4223-4229.
- Frank, W., Hoinkes, G., Purtscheller, F., Thoeni, M., Fluegel, H. W. and Faupl, P., 1987. The Austroalpine Unit West of the Hohe Tauern: The Oetztal-Stubai Complex as an Example for the Eoalpine Metamorphic Evolution. In: Fluegel, H. W. and Faupl, P. (eds.), *Geodynamics of the Eastern Alps*. Deuticke - Vienna, 179 - 225.
- Frisch, W., 1980. Post-Hercynian formations of the western Tauern window: sedimentological features, depositional environment, and age. *Mitteilungen der Österreichischen Geologischen Gesellschaft*, 71/72, 49-63.
- Frisch, W., Dunkl, I. and Kuhlemann, J., 2000. Post-collisional orogen-parallel large-scale extension in the Eastern Alps. *Tectonophysics*, 327, 239-265.
- Froitzheim, N., Conti, P. and van Daalen, M., 1997. Late Cretaceous, synorogenic, low-angle normal faulting along the Schlinig fault (Switzerland, Italy, Austria) and its significance for the tectonics of the Eastern Alps. *Tectonophysics*, 280, 267-293.
- Fügenschuh, B., Mancktelow, N. S. and Seward, D., 2000. Cretaceous to Neogene cooling and exhumation history of the Oetztal-Stubai basement complex, eastern Alps: A structural and fission track study. *Tectonics*, 19, 905-918.
- Fügenschuh, B., Seward, D. and Mancktelow, N., 1997. Exhumation in a convergent orogen: the western Tauern window. *Terra Nova*, 9, 213-217.

- Grasemann, B. and Mancktelow, N., 1993. Two-dimensional thermal modelling of normal faulting: the Simplon Fault Zone, Central Alps, Switzerland. *Tectonophysics*, 225, 155-165.
- Hoinkes, G.; Koller, F.; Rantitsch, G.; Dachs, E.; Hock, V.; Neubauer, F. and Schuster, R., 1999. Alpine metamorphism of the Eastern Alps. *Schweizerische Mineralogische und Petrographische Mitteilungen*, 79, 155-181.
- Koch, J. and Guenther, M., 1995. Relationship between random and maximum vitrinite reflectance. *Fuel*, 74, 1687- 691.
- Krainer, K., 1990. Ein Beitrag zum Oberkarbon der Steinacher Decke ("Karbon des Nößlacher Joches", Tirol). *Mitteilungen der Gesellschaft der Geologie- und Bergbaustudenten in Österreich*, 36, 87-99.
- Krainer, K., 1992. Fazies, Sedimentationsprozesse und Paläogeographie im Karbon der Ost- und Südalpen. *Jahrbuch der Geologischen Bundesanstalt*, 135, 99-193.
- Lahfid, A., Beyssac, O., Deville, E., Negro, F., Chopin, C. and Goffe, B., 2010. Evolution of the Raman spectrum of carbonaceous material in low-grade metasediments of the Glarus Alps (Switzerland). *Terra Nova*, 22, 354-360.
- Lünsdorf, N. K., 2010. The Comparability of Raman Data of Carbonaceous Material - A Systematical Approach to Uncertainties in Measurements and Evaluation. Master thesis, Georg-August-Universität Göttingen, Göttingen, unpublished, 148 pp.
- Neubauer, F., Genser, J., Kurz, W. and Wang, X., 1999. Exhumation of the Tauern window, Eastern Alps. *Physics and Chemistry of the Earth, Part A-solid Earth and Geodesy*, 24, 675-680.
- Rantitsch, G., Grogger, W., Teichert, C., Ebner, F., Hofer, C., Maurer, E. M., Schaffer, B. and Toth, M., 2004. Conversion of carbonaceous material to graphite within the Greywacke Zone of the Eastern Alps. *International Journal of Earth Sciences*, 93, 959-973.
- Rantitsch, G., Sachsenhofer, R. F., Hasenhuttl, C., Russegger, B. and Rainer, T., 2005. Thermal evolution of an extensional detachment as constrained by organic metamorphic data and thermal modelling: Graz Paleozoic Nappe Complex (Eastern Alps). *Tectonophysics*, 411, 57-72.
- Rantitsch, G. and Judik, K., 2009. Alpine metamorphism in the central segment of the Western Greywacke Zone (Eastern Alps). *Geologica Carpathica*, 60, 319-329.
- Reiners, P.W., 2005. Zircon (U-Th)/He thermochronometry. *Reviews in Mineralogy & Geochemistry*, 58, 151-179.
- Reiter, F., Lenhardt, W. A. and Brandner, R., 2005. Indications for activity of the Brenner Normal Fault zone (Tyrol, Austria) from seismological and GPS data. *Austrian Journal of Earth Sciences*, 97, 16-23.
- Rockenschaub, M., Kolenprat, B. and Frank, W., 2003. Geochronologische Daten aus dem Brennergebiet: Steinacher Decke, Brennermesozoikum, Ötz-Stubai-Kristallin, Innsbrucker Quarzphyllitkomplex, Tarntaler Mesozoikum. *Arbeitstagung 2003: Blatt 148 Brenner*, Geologische Bundesanstalt.
- Rockenschaub, M. and Nowotny, A., 2009. Geologische Karte der Republik Österreich 1 : 50000 – Blatt 148 Brenner. *Geologische Bundesanstalt*, Wien.
- Rosenberg, C. and Garcia, S., 2011. Estimating displacement along the Brenner Fault and orogen-parallel extension in the Eastern Alps. *International Journal of Earth Sciences*, 1-17.
- Schmid, S. M., Fügenschuh, B., Kissling, E. and Schuster, R., 2004. Tectonic map and overall architecture of the Alpine orogen. *Eclogae Geologicae Helveticae*, 97, 93-117.
- Schulz, O. and Fuchs, H. W., 1991. Kohle in Tirol: Eine historische, kohlenpetrologische und lagerstättenkundliche Betrachtung. *Archiv für Lagerstättenforschung der geologischen Bundesanstalt*, 13, 123 – 213.
- Selverstone, J., 1988. Evidence for east-west crustal extension in the Eastern Alps – Implications for the unroofing history of the Tauern Window. *Tectonics*, 7, 1, 87 – 105.
- Selverstone, J., Axen, G. J. and Bartley, J. M., 1995. Fluid inclusion constraints on the kinematics of footwall uplift beneath the Brenner-line Normal-fault, Eastern Alps. *Tectonics*, 14, 264-278.
- Wang, Y., Alsmeyer, D. C. and McCreery, R. L., 1990. Raman spectroscopy of Carbon Materials - Structural Basis of Observed Spectra. *Chemistry of Materials*, 2, 557-563.
- Wojdyr, M., 2010. Fityk: a general-purpose peak fitting program. *Journal of Applied Crystallography*, 43, 1126-1128.

Received: 14 June 2011

Accepted: 31 July 2012

N. Keno LÜNSDORF<sup>1)</sup>, István DUNKL<sup>1)</sup>, Burkhard C. SCHMIDT<sup>2)</sup>, Gerd RANTITSCH<sup>3)</sup> & Hilmar von EYNATTEN<sup>1)</sup>

<sup>1)</sup> Dept. of Sedimentology & Environmental Geology, Geoscience Center Georg-August-Universität Göttingen, Germany;

<sup>2)</sup> Dept. of Experimental & Applied Mineralogy, Geoscience Center Georg-August-Universität Göttingen, Germany;

<sup>3)</sup> Department of Applied Geosciences and Geophysics, University of Leoben, Austria;

<sup>\*)</sup> Corresponding author, keno.luensdorf@geo.uni-goettingen.de